Off-Grid High Resolution DOA Estimation for GNSS Circular Array Receivers

Xiangrong Wang[#*], Elias Aboutanios[#], Moeness Amin[*], Chow Yii Pui[+]

[#]*School of Electrical Engineering, University of New South Wales, NSW 2052, Australia*

[*]*Center for Advanced Communications, Villanova University, PA 19085, USA*

[+]*School of Electrical & Electronic Engineering, University of Adelaide, South Australia, Australia*

1. BIOGRAPHY

Xiangrong Wang received both the Bachelor and Master degrees in electrical engineering from Nanjing University of Science and Technology, China, in 2009 and 2011, respectively. She is working toward the Ph.D. degree in electrical engineering in University of New South Wales, Sydney, Australia. She is currently a visiting research student in the Center for Advanced Communications, Villanova University. Her research interests include adaptive array processing, array beampattern synthesis, DOA estimation and convex optimization.

2. ABSTRACT

Direction of Arrival (DOA) estimation using antenna arrays is an important problem for combating jamming in GPS, as accurate DOA estimates lead to better interference suppression. In this paper, we improve the estimation DOA accuracy when the true incident angles are off the discretised sampling grid points. We propose a bisection interpolation method based on MUSIC pseudo-spatial spectrum coefficients. The proposed method can be applied to multiple uncorrelated sources in the field of view without any constraints on the antenna array shape. For coherent sources, both beamspace transformation and spatial smoothing are utilised to decorrelate the signals for uniform circular arrays, with sufficient number of antennas, prior to dichotomous search. Both simulated and experimental results validate the effectiveness and efficiency of the proposed algorithm.

3. INTRODUCTION

Global navigation satellite systems (GNSS) receivers are vulnerable to the presence of interference. In order to counter this problem, antenna arrays are proposed to enhance the performance of GNSS receivers by steering nulls towards the interfering signals, [1] [2], [3], [4], [5]. Thus, accurate DOA estimates are important for desirable null formation. There has been extensive research on high-resolution DOA estimation techniques, such as maximum likelihood technique and MUSIC algorithm. The main advantage of using MUSIC, rather than a maximum likelihood estimator, is its relative computational simplicity. Unfortunately, MUSIC is applicable only when the sources are either uncorrelated or partially correlated. There exist situations where the signals become coherent or almost coherent, such as multipath propagation or deliberately introduced coherent signals by smart jammers in GPS scenarios. In [6], an effective spatial smoothing technique for uniform linear arrays (ULA) was introduced to restore the dimensionality of the signal subspace. In order to apply spatial smoothing techniques to arbitrary shaped arrays, Friedlander [7] proposed an interpolated array scheme that employed interpolation matrices to map the received signal of an arbitrary array onto that of a virtual ULA. However, different sets of interpolator coefficients are required to provide good estimates for different angle sectors. For uniform circular arrays (UCA), phase mode excitation-based beamforming is utilised to synthesize a beamspace manifold similar to that of a ULA under some conditions [8], [9], [10]. Afterwards, spatial smoothing techniques can be utilised to decorrelate coherent sources.

However, all the aforementioned methods assume that true DOAs are exactly on the discretised sampling grid points and suffer considerable performance degradation when the assumption is violated. Although employing sufficiently dense sampling grids is one solution to improve the estimation accuracy, this approach requires an extensive search, hence incurring a high computational cost. The off-grid DOA estimation problem was addressed in a number of ways, including the sparse total least-squares (STLS) approach [11], the Off Grid Sparse Bayesian Inference (OGSBI) method [12] and the Simultaneous Orthogonal Matching Pursuit Least-Squares (SOMP-LS) algorithm [13]. The obvious drawback of the STLS is its unrealistic model of Gaussian distributed off-grid errors. One shortcoming of the OGSBI is that up to 1000 iterations are required for high accuracy especially for dense sampling-grids due to the probabilistic property of the Bayesian inference method. The SOMP-LS method, on the other hand, offers fewer guarantees on the estimation accuracy and resolution capability.

There are various kinds of interpolators based on Fourier coefficients proposed in the literature to solve this problem as well. One simple and commonly used interpolator employs zero-padding for extended data vector. However, interpolating on every frequency component is not necessary, and the zero-padding interpolator gives fine resolution to spatial angular sectors of no jamming

activities. More importantly, achieving a frequency resolution that is comparable to the Cramer-Rao Lower Bound (CRLB) would require substantial padding, especially in high signal to noise ratio (SNR) cases, and result in excessive computational load. Interpolation using only the peak Fourier coefficient and its two neighbours is intuitively justified by the fact that most the "energy" of a sinusoidal signal is contained in these three samples [14], [15], [16], [17], [18]. However, all these interpolators based on Fourier coefficients are constrained in the ULA cases and suffer a low resolution capability due to the Rayleigh criterion. Most of the GPS multi-antenna receivers are Controlled Radiation Pattern Antenna (CRPA) arrays, which have a circular aperture with one element in the center and three to seven elements on the circumference. Therefore, these interpolation methods based on Fourier coefficients are not applicable for DOA estimation in GPS scenarios.

In order to estimate off-grid DOAs accurately and efficiently, we propose a bisection interpolation method based on MUSIC pseudo-spatial spectrum coefficients. The proposed method can be applied to multiple uncorrelated sources in the field of view without any constraints on the antenna array shape. For coherent sources impinging on the UCA with a certain number of antennas, beamspace transformation and spatial smoothing are utilised to decorrelate the signals prior to dichotomous search. We implement the proposed interpolation method in both simulated and real GPS experiments, where a 16-antenna UCA and an 8-antenna UCA were employed respectively. In order to validate the proposed bisection interpolation approach, we collect clean GPS data utilizing the 8-antenna UCA and inject interference signals with Matlab®, where their DOAs are off discretized sampling grid points. Both the simulation and experimental results prove that the proposed method can maintain accurate DOA estimates even under a set of coarse sampling grid points, thus reducing the computational complexity.

4. ANALYSIS OF UCA WITH AND WITHOUT A CENTER ANTENNA

In this section, we will analyse the UCA with and without an antenna in the center of the circle in terms of both the beampattern and DOA estimation variance. The geometry of an M-antenna UCA is depicted in Figure 1. The antenna elements are assumed to be identical and omnidirectional. There is one antenna located in the center (which we denote as the zeroth antenna) and other M-1 elements are uniformly distributed over the circumference of a circle of radius r in the x-y plane. Without loss of generality, we assume the first antenna is placed on the x axis, then the n_{th} antenna is displaced by an angle γ_n from the x axis,

$$\gamma_n = (\text{n-1})\gamma = 2\pi(\text{n-1})/(\text{M-1}), \text{n} = 1,...,\text{M}-1 \quad (1)$$

Here, $\gamma = 2\pi/(\text{M-1})$ is the angle between two consecutive antennas. Then, the position vector of the n_{th}, n=1,…,M-1 antenna is

$$\mathbf{p}_n = [\text{r}\cos\gamma_n, \text{r}\sin\gamma_n]^T. \quad (2)$$

First, we investigate the effect of the center antenna on the conventional beampattern of the UCA. We employ the 8-antenna experimental UCA, i.e., there are seven elements uniformly distributed over the circular circumference. The radius of the circle is one wavelength. The elevation angle is fixed at 0° without special notice in the paper. The beampatterns of the UCA with and without center antenna are shown in Figure 2. We can observe that both the mainlobe width and the peak sidelobe level are the same for the two UCAs, whereas the two sidelobes closest to the mainlobe are much lower for the UCA with the center antenna due to the filled aperture. Thus the UCA with an antenna in the center is generally preferred for anti-jamming.

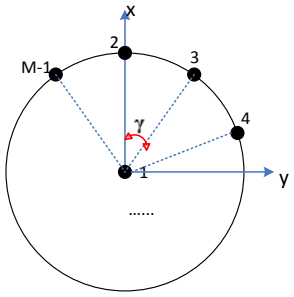

Figure 1 Uniform circular array geometry with one antenna in the center of the circle.

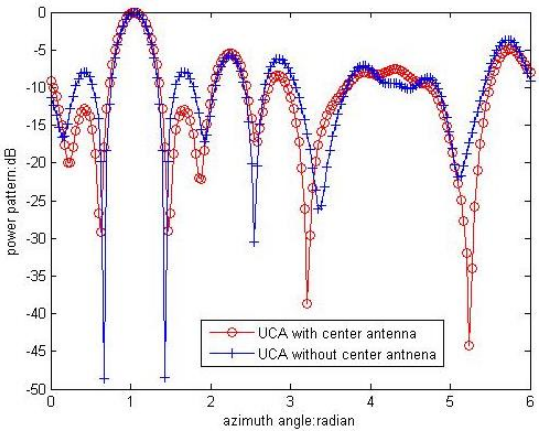

Figure 2 Conventional beampatterns of the UCA with and without center antenna.

Next, we investigate the effect of the center antenna on the DOA estimation performance. Theoretically, we show that the absence of the center antenna has a negligible effect on the CRLB of the UCA. As shown in [19], the CRLB is a function of the array geometry only through the "moments of inertia" of the array. The CRLB of the azimuth angle φ of a two-dimensional antenna array for a given elevation angle θ is

$$C_\varphi = \frac{1/M + \rho}{2\rho^2 k_0^2 \cos^2\theta(\sin^2\varphi Q_{xx} + \cos^2\varphi Q_{yy} - \sin 2\varphi Q_{xy})}, \quad (3)$$

where ρ is the SNR and $k_0 = 2\pi/\lambda$ is the wavenumber. The "moments of inertia" Q_{xx}, Q_{yy}, Q_{xy} of the UCA are defined as follows,

$$\text{Q}_{xx} = \sum_{\text{m=1}}^{\text{M}} (\text{x}_\text{m} - \text{x}_\text{c})^2, \text{Q}_{yy} = \sum_{\text{m=1}}^{\text{M}} (\text{y}_\text{m} - \text{y}_\text{c})^2, \quad (4)$$

$$Q_{xy} = \sum_{m=1}^{M} (x_m - x_c)(y_m - y_c), \quad (5)$$

where x_m, y_m denote the x and y coordinates of the m_{th} antenna respectively. Regardless of whether the UCA has a center antenna or not, its gravity center, x_c, y_c is actually the circular center, i.e.

$$x_c = r\sum_{m=2}^{M} \cos\gamma_m = r\sum_{m=2}^{M} \cos\frac{2\pi(m-2)}{M-1} = 0, \quad (6)$$

$$y_c = r\sum_{m=2}^{M} \sin\gamma_m = r\sum_{m=2}^{M} \sin\frac{2\pi(m-2)}{M-1} = 0. \quad (7)$$

Therefore, according to Equations (4), (5), the "moments of inertia" of the UCA, in the two cases with and without the center antenna, are essentially the same. Accordingly, the difference of the CRLB between the two UCAs with and without the center antenna is,

$$\Delta C_\varphi = \frac{1}{2M(M-1)\rho^2 k_0^2 \cos^2\theta(\sin^2\varphi Q_{xx} + \cos^2\varphi Q_{yy} - \sin 2\varphi Q_{xy})}, \quad (8)$$

We can see from Equation (8) that the CRLB difference is negligible, which is also verified by experimental results in Section 7. In essence, the UCA with a center antenna is beneficial for interference nulling, whereas the additional center antenna does not improve the DOA estimation performance. Moreover, as shown in Section 5, the existence of the center antenna, makes the transformation to a virtual ULA inefficient. Therefore, in an open-loop null steering algorithm [20], [21], the UCA without the center antenna is preferred for DOA estimation, especially in the case with coherent sources, and the center antenna can be considered for the follow-on interference nulling.

5. MUSIC ALGORITHM AND FORWARD SPATIAL SMOOTHING FOR UCA

Since the proposed method interpolates off-grid DOAs based on the peak spatial spectrum coefficients and positions, a complete estimation procedure is comprised of two steps. In the first step, an initial DOA estimation is implemented utilising coarse estimation algorithms in order to obtain the number of estimated sources and their peak grid positions. Then a fine search, i.e. interpolation, is adopted in the second step to increase the estimation accuracy. Thus it is intuitive to conclude that the resolution capability and robustness against coherent signals of the proposed method have a great dependence on the first estimation step. We adopt the MUSIC algorithm in the first step, since it is capable of resolving two closely spaced or highly correlated signals (with spatial smoothing) even at low SNR cases, we adopt it in the first step.

Let us assume there are K far-field stationary narrowband signals impinging on the UCA with elevation and azimuth $\boldsymbol{\theta} = [\theta_1, \theta_2, ..., \theta_K]$ and $\boldsymbol{\varphi} = [\varphi_1, \varphi_2, ..., \varphi_K]$ respectively. The steering vector of the k_{th} source is

$$\mathbf{a}_k = [1, e^{j\zeta_k \cos(\varphi_k - \gamma_2)}, ..., e^{j\zeta_k \cos(\varphi_k - \gamma_M)}]^T, \quad (9)$$

where $\zeta_k = (2\pi/\lambda) r\cos\theta_k$ and $()^T$ is the transpose operation. The center antenna is included in Equation (9). The received signal can be expressed as,

$$\mathbf{x}(t) = \sum_{k=1}^{K} \mathbf{a}_k s_k(t) + \mathbf{n}(t) = \mathbf{A}\mathbf{s}(t) + \mathbf{n}(t), t = 1, ..., T \quad (10)$$

where

$$\mathbf{s}(t) = [s_1(t), s_2(t), ..., s_K(t)]^T, \quad (11)$$

is the received signal complex amplitude and $\mathbf{n}(t)$ is the white noise vector, uncorrelated with the source signals. The steering matrix is defined as,

$$\mathbf{A} = [\mathbf{a}_1, \mathbf{a}_2, ..., \mathbf{a}_K], \quad (12)$$

with $\mathbf{a}_k$ being the steering vector of the k_{th} signal defined in Equation (9). The array covariance matrix $\mathbf{R}$ can be approximated as

$$\mathbf{R} \approx \sum_{t=1}^{T} \mathbf{x}(t)\mathbf{x}^H(t) = \mathbf{A}\mathbf{S}\mathbf{A}^H + \sigma^2\mathbf{I}, \quad (13)$$

where $\mathbf{S}$ is the source covariance matrix defined as

$$\mathbf{S} \approx \sum_{t=1}^{T} \mathbf{s}(t)\mathbf{s}^H(t), \quad (14)$$

where σ^2 is the variance of the additive noise and $\mathbf{I}$ is an identity matrix. $()^H$ is the transpose conjugate operation. Taking eigenvalue decomposition of $\mathbf{R}$ yields,

$$\mathbf{R} = \mathbf{E}\boldsymbol{\Sigma}\mathbf{E}^H, \quad (15)$$

Under the condition of no coherent or highly correlated sources, the signal covariance matrix $\mathbf{S}$ becomes full rank. The noise eigenvector matrix is

$$\mathbf{E}_n = [\mathbf{e}_{K+1}, \mathbf{e}_{K+2}, ..., \mathbf{e}_M], \quad (16)$$

where the columns are the eigenvectors corresponding to the M-K smallest eigenvalues. For a fixed elevation angle, let $[\varphi_1, ..., \varphi_L]$ be a uniform sampling grid over the range $[0^\circ, 360^\circ]$. In this case the unit grid interval is 360/L degrees. The MUSIC measurement is chosen to be

$$M(\theta, \varphi_l) = [\mathbf{a}(\theta, \varphi_l)^H (\mathbf{E}_n \mathbf{E}_n^H) \mathbf{a}(\theta, \varphi_l)]^{-1}, l = 1, ..., L \quad (17)$$

The K values at which $M(\theta, \varphi)$ is maximized are taken as the rough estimates of the DOAs in the first step.

When the source covariance matrix $\mathbf{S}$ is singular, the MUSIC algorithm in Equation (10) would fail. A pre-processing scheme, called spatial smoothing, introduced in [6] can restore the rank of $\mathbf{S}$, even when the signals are coherent. Since spatial smoothing techniques were initially developed for ULAs, for UCAs, phase mode excitation-based beamforming can be utilised to transform the received signal to that of a virtual array whose structure is amenable to the application of spatial smoothing. The transformation procedure is detailed as follows.

First, according to [9], a rule of thumb for determining the maximum number of mode order, H, is

$$H \geq \frac{2\pi}{\lambda} r. \quad (18)$$

For example, a UCA with radius $r = \lambda$, the maximum mode order is H=6. In other word, the number of sensors in the virtual ULA is 2H+1 = 13.

By omitting the center antenna and considering the M-1 antennas on the circumference, the normalized beam-forming weight vector, which excites the array with phase mode h, |h|<=H is

$$\mathbf{w}_h^H = \frac{1}{\sqrt{M-1}}[1, e^{j2\pi h/(M-1)}, ..., e^{j2\pi h(M-2)/(M-1)}], \quad (19)$$

The resulting beampattern for the k_{th} source is then

$$f_h = \mathbf{w}_h^H \mathbf{a}_k = \frac{1}{\sqrt{M-1}} (\sum_{n=2}^{M} e^{jh\gamma_n} e^{j\zeta_k \cos(\varphi_k - \gamma_n)}), \quad (20)$$

When the number of physical antennas,

$$M > 2H+1, \quad (21)$$

the array pattern can be approximated as,

$$f_h \approx \sqrt{M-1}\, j^h J_h(\zeta_k) e^{jh\varphi_k}, \quad (22)$$

where $J_h(\zeta_k)$ is the Bessel function of the first kind of order h.

The beamforming matrix **F** is defined, from Equation (19), as, [9], [10]

$$\mathbf{F} = \frac{1}{\sqrt{M-1}} \begin{bmatrix} 1 & e^{-j2\pi H/(M-1)} & ... & e^{-j2\pi H(M-2)/(M-1)} \\ ... & ... & ... & ... \\ 1 & e^{-j2\pi/(M-1)} & ... & e^{-j2\pi(M-2)/(M-1)} \\ 1 & 1 & ... & 1 \\ 1 & e^{j2\pi/(M-1)} & ... & e^{j2\pi(M-2)/(M-1)} \\ ... & ... & ... & ... \\ 1 & e^{j2\pi H/(M-1)} & ... & e^{j2\pi H(M-2)/(M-1)} \end{bmatrix}, \quad (23)$$

The beamspace steering vector, $\tilde{\mathbf{a}}_k$, synthesized by **F** is thus,

$$\tilde{\mathbf{a}}_k = \mathbf{F}\mathbf{a}_k = \mathbf{J}\mathbf{v}_k, \quad (24)$$

where the matrix **J** is diagonal, i.e.,

$$\mathbf{J} = \sqrt{M-1}\, \mathrm{diag}\{j^{-H} J_{-H}(\zeta_k), ..., j^0 J_0(\zeta_k), ..., j^H J_H(\zeta_k)\}, \quad (25)$$

To preserve only the angle-dependent phase, which is our goal, we multiply $\tilde{\mathbf{a}}_k$ by the inverse diagonal matrix $\mathbf{J}^{-1}$ which yields

$$\hat{\mathbf{a}}_k = \mathbf{J}^{-1}\tilde{\mathbf{a}}_k = \mathbf{J}^{-1}\mathbf{F}\mathbf{a}_k = \mathbf{v}_k, \quad (26)$$

where $\mathbf{v}_k$ is a 2H+1 dimensional vector,

$$\mathbf{v}_k = [e^{-jH\varphi_k}, ..., 1, ..., e^{jH\varphi_k}]^T, \quad (27)$$

It is clear from Equation (27) that the M-antenna UCA is transformed to a virtual 2H+1-antenna ULA. Spatial smoothing can then be utilized to decorrelate the coherent signals. In this paper, we adopt a forward spatial smoothing method as follows.

Firstly, received signals **x**(t) in Equation (10) are transformed to those of a virtual ULA, i.e.

$$\mathbf{y}(t) = \mathbf{J}^{-1}\mathbf{F}\mathbf{x}(t), t = 1, ..., T \quad (28)$$

Then, the virtual ULA of 2H+1 sensors is divided into overlapping sub-arrays of size H_0, with the first sub-array formed from the sensors $\{1,\ldots,H_0\}$ and the second sub-array formed from the sensors $\{2,\ldots,H_0+1\}$ and so on. The spatially smoothed covariance matrix, with $L=2H+2-H_0$ smoothing steps, is

$$\tilde{\mathbf{R}} = \frac{1}{L}\sum_{p=1}^{L} \mathbf{R}_p, \quad (29)$$

where $\mathbf{R}_p$ is the covariance matrix of the p_{th} sub-array, i.e.,

$$\mathbf{R}_p = \frac{1}{T}(\mathbf{Y}_{p:p+H_0-1}\mathbf{Y}_{p:p+H_0-1}^H), \quad (30)$$

where $\mathbf{Y} = [\mathbf{y}(1), \mathbf{y}(2), ..., \mathbf{y}(T)]$ and $\mathbf{Y}_{p:p+H_0-1}$ is obtained by extracting from the p_{th} row to the $(p+H_0-1)_{th}$ row. It should be noted that the number of sub-arrays, L, must equal to the degree of the largest coherent signal group [6].

6. BISECTION INTERPOLATION BASED ON MUSIC PSEUDO-SPECTRUM COEFFICIENTS

It is hard to derive a closed formula for the true off-grid value from the MUSIC pseudo-spectrum; thus we implement an iterative search where we halve interpolation step length at each iteration. The proposed bisection interpolation method is similar to the Dichotomous search in [16], with the difference that the latter is based on Fourier coefficients. Below, we elaborate on implementation procedures of the proposed bisection interpolation method in both cases of uncorrelated and coherent sources.

6.1 BISECTION INTERPOLATION FOR UNCORRELATED SIGNALS

In the case of uncorrelated signals, the MUSIC algorithm can be applied directly based on the circular array as shown in Equations (15), (16), (16 with the center antenna included. Let us assume that the K peak positions estimated from the first step of MUSIC search as $\hat{k}_i, i = 1, ..., K$. Since most of the interferences are descending from the horizontal direction in GPS, we fix the elevation angle to be 0°. Then the implementation procedure of bisection interpolation method in the case of uncorrelated signals is as follows:

Step 0: Initialize the threshold value τ (for example 0.01), $\delta_1 = 0.5$ and $\delta_2 = -0.5$;

For each estimated signal i=1,..,K, iterate

Step 1: Calculate the two shifted azimuth angles:

$$\varphi_i^1 = 360(\hat{k}_i + \delta_1 - 1)/L, \quad (31)$$

$$\varphi_i^2 = 360(\hat{k}_i + \delta_2 - 1)/L, \quad (32)$$

and the corresponding shifted steering vectors are

$$\mathbf{a}_i^1 = [1, e^{j\zeta_i \cos(\varphi_i^1 - \gamma_2)}, ..., e^{j\zeta_i \cos(\varphi_i^1 - \gamma_M)}]^T, \quad (33)$$

$$\mathbf{a}_i^2 = [1, e^{j\zeta_i \cos(\varphi_i^2 - \gamma_2)}, ..., e^{j\zeta_i \cos(\varphi_i^2 - \gamma_M)}]^T, \quad (34)$$

Step 2: Calculate the pseudo-spectrum coefficients:

$$b_1 = \frac{1}{\mathbf{a}_i^{1H}(\mathbf{E}_n\mathbf{E}_n^H)\mathbf{a}_i^1}, b_2 = \frac{1}{\mathbf{a}_i^{2H}(\mathbf{E}_n\mathbf{E}_n^H)\mathbf{a}_i^2}, \quad (35)$$

Step 3: Let $\Delta = b_1 - b_2$. Update δ_1 and δ_2 as follows:

a) If $\Delta \le -\tau$, then $\delta_1 = 0.5(\delta_1 + \delta_2)$ and $\delta_2 = \delta_2$, go back to Step 2;

b) If $\Delta \geq \tau$, then $\delta_2 = 0.5(\delta_1 + \delta_2)$ and $\delta_1 = \delta_1$, go back to Step 2;

c) Otherwise, terminate the iteration with $\hat{\delta} = 0.5(\delta_1 + \delta_2)$ and obtain the true DOA of the i_{th} signal as $\varphi_i = 360(\hat{k}_i + \hat{\delta})/L$.

It should be noted that the value of the off-grid parameter δ is within the range [-0.5, 0.5] around the peak position.

6.2 BISECTION INTERPOLATION FOR COHERENT SIGNALS

For coherent sources, both beamspace transformation and spatial smoothing are required prior to DOA estimation, per Equations (28), (29), (30). Implementing the eigenvalue decomposition on the spatially smoothed covariance matrix $\tilde{\mathbf{R}}$ in Equation (28) yields the noise subspace,

$$\tilde{\mathbf{E}}_n = [\tilde{\mathbf{e}}_{K+1}, \tilde{\mathbf{e}}_{K+2}, ..., \tilde{\mathbf{e}}_{2H+2-2K}], \quad (36)$$

where each eigenvector $\tilde{\mathbf{e}}_k$ is of dimension 2H+2-K. Performing searching in the azimuth range [0°, 360°], we obtain the MUSIC measurements,

$$\tilde{M}(\theta, \varphi_l) = [\tilde{\mathbf{a}}(\theta, \varphi_l)^H (\tilde{\mathbf{E}}_n \tilde{\mathbf{E}}_n^H) \tilde{\mathbf{a}}(\theta, \varphi_l)]^{-1}, l = 1, ..., L \quad (37)$$

where $\tilde{\mathbf{a}}(\theta, \varphi_l)$ is the transformed beamspace steering vector, i.e.

$$\tilde{\mathbf{a}}(\theta, \varphi_l) = [e^{-jH\varphi_l}, ..., 1, ..., e^{j(H+1-K)\varphi_l}]^T, \quad (38)$$

Assume the K estimated peak positions as $\hat{k}_i, i = 1, ..., K$. Then, the implementation procedure of the bisection interpolation method in the case of coherent sources is as follows:

Step 0: Initialize the threshold value τ (for example 0.01), $\delta_1 = 0.5$ and $\delta_2 = -0.5$;

For each estimated signal i=1,..,K, iterate

Step 1: Calculate the two shifted azimuth angles:

$$\varphi_i^1 = 360(\hat{k}_i + \delta_1 - 1)/L, \quad (39)$$

$$\varphi_i^2 = 360(\hat{k}_i + \delta_2 - 1)/L, \quad (40)$$

and the corresponding shifted steering vectors are

$$\tilde{\mathbf{a}}_i^1 = [e^{-jH\varphi_i^1}, ..., 1, ..., e^{j(H+1-K)\varphi_i^1}]^T, \quad (41)$$

$$\tilde{\mathbf{a}}_i^2 = [e^{-jH\varphi_i^2}, ..., 1, ..., e^{j(H+1-K)\varphi_i^2}]^T, , \quad (42)$$

Step 2: Calculate the pseudo-spectrum coefficients:

$$b_1 = \frac{1}{\tilde{\mathbf{a}}_i^{1H} (\tilde{\mathbf{E}}_n \tilde{\mathbf{E}}_n^H) \tilde{\mathbf{a}}_i^1}, b_2 = \frac{1}{\tilde{\mathbf{a}}_i^{1H} (\tilde{\mathbf{E}}_n \tilde{\mathbf{E}}_n^H) \tilde{\mathbf{a}}_i^1}, \quad (43)$$

Step 3: Let $\Delta = b_1 - b_2$. Update δ_1 and δ_2 as follows:

a) If $\Delta \leq -\tau$, then $\delta_1 = 0.5(\delta_1 + \delta_2)$ and $\delta_2 = \delta_2$, go back to Step 2;

b) If $\Delta \geq \tau$, then $\delta_2 = 0.5(\delta_1 + \delta_2)$ and $\delta_1 = \delta_1$, go back to Step 2;

c) Otherwise, terminate the iteration with $\hat{\delta} = 0.5(\delta_1 + \delta_2)$ and obtain the true DOA of the i_{th} signal as $\varphi_i = 360(\hat{k}_i + \hat{\delta})/L$.

7. SIMULATION AND EXPERIMENTAL RESULTS

In this section, both simulation and experimental results are presented to validate the effectiveness of the proposed method. The experimental array has one antenna in the center and seven antennas uniformly distributed over the circular circumference with the radius of one wavelength. According to the condition in Equation (21), the number of antennas should be greater than 15 in order to guarantee the accuracy of the transformation. Therefore, we assume a 16-antenna UCA for the simulation with one antenna in the center and the remaining 15 elements are placed on the circumference. To be consistent with the theory, the elevation angle is fixed to be 0° in both simulation and experiment.

7.1 THE CASE OF UNCORRELATED SIGNALS

Firstly, we validate the theory that the center antenna in the UCA does not affect the DOA estimation performance by utilizing the experimental 8-antenna UCA in the case of a single source. The number of snapshots is set to be 200 and that of the sampling grid points is 90. The arrival angle of the source is uniformly distributed within the range $2\pi/90*[29.5, 30.5]$ in each run. The estimation variance versus different values of SNR are plotted in Figure 3 for the two cases with and without the center antenna. Each point in Figure 3 is averaged by 200 Monte Carlo simulations. We also plot the CRLBs of the two UCAs for reference. We can observe that the estimation variance asymptotically approaches the CRLB when the SNR exceeds some threshold value. This result verifies the effectiveness of the proposed method. It is evident that the CRLB of the UCA with the center antenna is almost identical to that of the array without the center antenna, which verifies the theory developed in the section 4. Further, the estimation variances for the two cases are similar. Since the center antenna only affects the beamspace transformation in coherent signal environment, we omit it when dealing with DOA estimation of coherent sources.

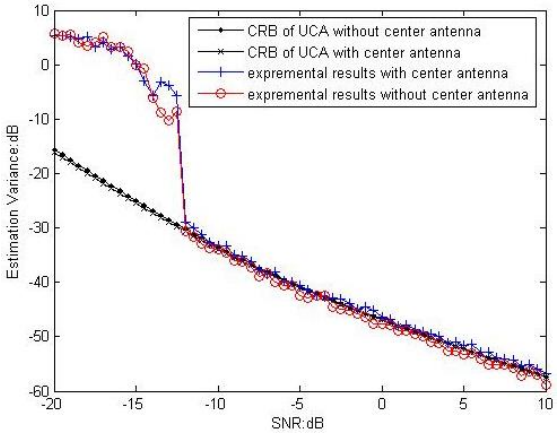

Figure 3 Estimation variance of experimental UCA with and without the center antenna.

We proceed to demonstrate that the proposed bisection interpolation method works well, even under a set of very coarse searching grid points. Simulation results of a 16-antenna UCA and experimental results of an 8-antenna UCA are both shown in Figure 4. The number of searching grid points is changing from 8 to 180 in steps of 4. The SNR is set to be 0dB and the number of snapshots is 200. Each point of the curve in Figure 4 is obtained by averaging 200 Monte Carlo runs. The off-grid offset δ is uniformly distributed within the range [-0.5, 0.5] in each run. We can see that when the number of searching grid points is greater than 12, the estimation variance becomes nearly constant for the 16-antenna UCA, whereas this threshold value increases to 16 for the 8-antenna UCA. However, both curves verify the fact that the proposed bisection interpolation method is effective under a set of very coarse searching grid points.

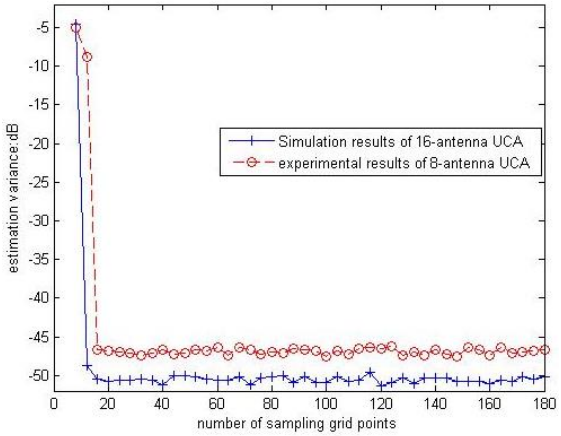

Figure 4 Estimation variance versus the number of searching grid points in the case of single source.

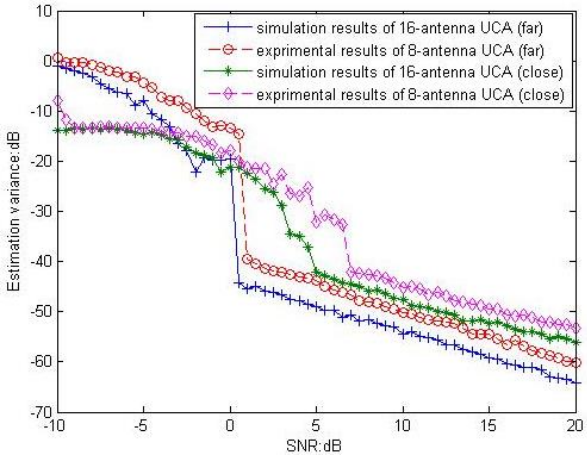

Figure 5 DOA estimation variance versus SNR in the case of two uncorrelated signals.

Finally, we present the curve of DOA estimation variance versus the SNR in the case of two uncorrelated signals. We consider two scenarios where the first signal is incident from the interval $[29.5, 30.5]\Delta\varphi$ with $\Delta\varphi = 2\pi/90$ and the second source is incident from $[44.5, 45.5]\Delta\varphi$ for widely separated sources and $[33.5, 34.5]\Delta\varphi$ for closely spaced sources. The number of time snapshots is 200 and also 200 Monte Carlo simulations are averaged to obtain the curve shown in Figure 5. It is clear that the estimation variance is much higher in the scenario where the two sources are closely spaced. More importantly, it demonstrates the effectiveness of the proposed bisection interpolation method in two typical scenarios when the SNR is larger than the threshold value for both the 16-antenna and 8-antenna UCAs.

7.2 THE CASE OF COHERENT SIGNALS

We again consider two scenarios of widely and closely separated sources, with the difference that the two sources are coherent. Figure 6 presents the normalized pseudo-spatial spectrum of two coherent signals based on the 16-antenna UCA utilizing the Bisection Interpolation method. Both signals have the same power and the SNR is set to be 20dB. The number of snapshots is 200 and that of searching grid points is 90. Each point of the spatial spectrum in Figure 6 is obtained by averaging 200 Monte-Carlo simulations. It is clear that, for widely separated coherent sources, where true DOAs are deviated from the discretized sampling grid points, the proposed bisection interpolation method can obtain accurate estimates. The method fails for the closely spaced source case. Thus, compared to the case of uncorrelated signals, the spatial resolution of the proposed method is decreased when the sources are coherent.

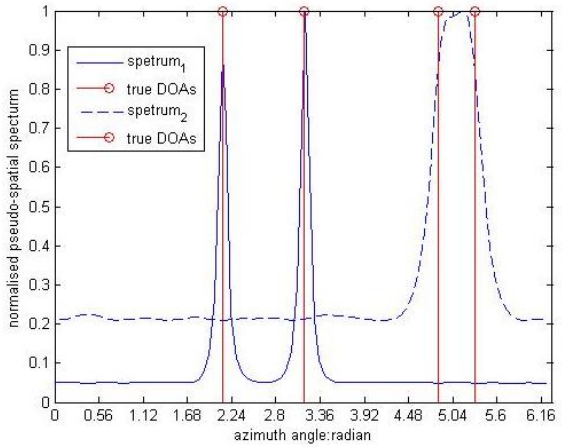

Figure 6 Normalized spatial spectrum of two coherent signals utilizing the Bisection Interpolation method.

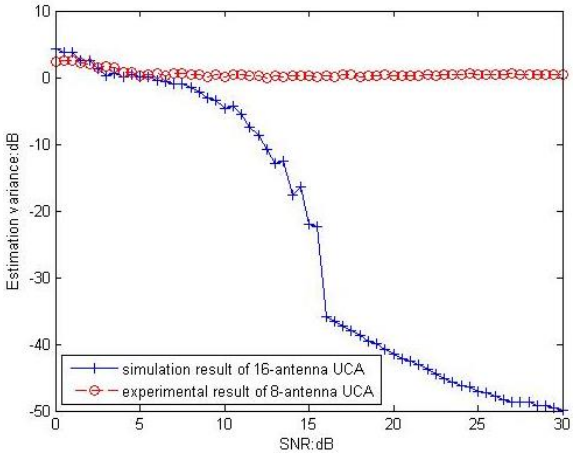

Figure 7 DOA estimation variance versus SNR in the case of coherent signals.

Next, we plot the curve of DOA estimation variance versus the SNR using two UCAs in the case of coherent signals. We set the first signal to come from the interval $[29.5, 30.5]\Delta\varphi$ with $\Delta\varphi = 2\pi/90$ and the second source is coming from $[44.5, 45.5]\Delta\varphi$. The number of snapshots is 200 and 200 Monte Carlo simulations are averaged to obtain the curve as shown in Figure 7. Firstly, we can see that the 16-antenna UCA works well when the SNR exceeds 16dB, which is much higher than the threshold of 0.5dB for the case of two uncorrelated signals. Secondly, the 8-antenna experimental UCA cannot distinguish the two coherent sources, because the number of antennas does not satisfy the condition in Equation (21).

Finally, we investigate the efficiency of the proposed method. The average computational time of estimating two coherent sources is 0.0048 seconds with 90 searching grid points and 200 time snapshots, which is much faster than the SBI-SVD method, which needs average 0.2 seconds for a similar example in [12].

8. CONCLUSIONS

A Bisection Interpolation method based on MUSIC pseudo-spatial spectrum coefficients was for off-grid DOA estimation. The proposed method can be applied to arbitrarily shaped antenna arrays in the case of uncorrelated sources. For coherent signals, a beamspace transformation and spatial smoothing were utilised to decorrelate the signals for UCAs prior to dichotomous search. It is verified by both the simulation and experimental results that the proposed method is capable of handling coherent signals and work well even under a set of very coarse searching grid points. Since GNSS receivers are very vulnerable to the interference and multipath signals, more accurate jammer localization can result in better cancellation, therefore enhancing the receiver performance. It should be noted that the transformation of UCAs to corresponding ULAs requires a certain number of antennas. This may place a challenge for typical GPS receivers.

9. ACKNOWLEDGMENTS

The authors would like to thank Mr. Matthew Trinkle of University of Adelaide for providing the experimental data.

10. REFERENCES

[1] Zhang Y.D. and Amin, M.G. (2001). Array processing for nonstationary interference suppression in DS/SS communications using subspace projection techniques. *IEEE Transactions on Signal Processing*, 49(12), 3005-3014.

[2] Amin, M.G. and Sun, W. (2005). A novel interference suppression scheme for global navigation satellite systems using antenna array. *IEEE Journal on Selected Areas in Communications*, 23(5), 999-1012.

[3] Sun, W. and Amin, M.G. (2005). A self-coherence anti-jamming GPS receiver. *IEEE Transactions on Signal Processing*, 53(10), 3910-3915.

[4] Friedlander, B. and Porat, B., (1989). Performance analysis of a null-steering algorithm based on direction-of-arrival estimation. *IEEE Transactions on Acoustics, Speech and Signal Processing*, 37(4), 461-466.

[5] Amin, M.G. (1992). Concurrent nulling and locations of multiple interferences in adaptive antenna arrays. *IEEE Transactions on Signal Processing*, 40(11), 2658-2668.

[6] Evans, J. E., Johnson, J.R. and Sun, D. F. (1982). Application of advanced signal processing techniques to angle of arrival estimation in ATC navigation and surveillance system. *Report 582, M.I.T. Lincoln Lab., Lexington, MA, 1982.*

[7] Friedlander, B. and Weiss, A.J. (1994). Direction finding using spatial smoothing with interpolated arrays. *IEEE Transactions on Aerospace and Electronic Systems*, 28(2), 574-587.

[8] Tewfik, A.H. and Hong, W. (1992). On the application of uniform linear array bearing estimation techniques to uniform circular arrays. *IEEE Transactions on Signal Processing*, 40(4), 1008-1011.

[9] Wax, M. and Sheinvald, J. (1994). Direction finding of coherent signals via spatial smoothing for uniform circular arrays. *IEEE transactions on antennas and propagation*, 42(5), 613-620.

[10] Mathews, C. P. and Zoltowski, M.D. (1994). Eigenstructure techniques for 2-D angle estimation with uniform circular arrays. *IEEE Transactions on Signal Processing*, 42(9), 2395-2407.

[11] Zhu H., Leus G. and Giannakis G. (2011). Sparsity cognizant total least-squares for perturbed compressive sampling, *IEEE Transactions on Signal processing*, 59(5), 2002-2016.

[12] Yang Z., Xie L. and Zhang C. (2013). Off-Grid Direction of Arrival Estimation Using Sparse Bayesian Inference. *IEEE Transactions on Signal Processing*, 61(1), 38-43.

[13] Gretsistas A. and Plumbley M. (2012). An alternating descent algorithm for the off-grid DOA estimation problem with sparsity constraints. *The proceeding of the 20th European Signal Processing Conference (Eusipco)*, 874-878.

[14] Aboutanios, E. and Mulgrew, B. (2005). Iterative frequency estimation by interpolation on Fourier coefficients. *IEEE Transactions on Signal Processing*, 53(4), 1237-1242.

[15] Aboutanios, E. (2010). Generalised DFT-based estimators of the frequency of a complex exponential in noise. *2010 3rd International Congress on Image and Signal Processing (CISP)*, 2998-3002.

[16] Aboutanios, E. (2004). A modified dichotomous search frequency estimator. *IEEE Signal Processing Letters*, 11(2), 186-188.

[17] Macleod, M.D. (1998). Fast nearly ML estimation of the parameters of real or complex single ones or resolved multiple tones. *IEEE Transactions on Signal Processing*, 46(1), 141-148.
[18] Provencher, S. (2011). Parameters Estimation of Complex Multi-tone Signal in the DFT Domain. *IEEE Transactions on Signal Processing*, 59(7), 3001-3012.
[19] Dogandzic, A. and Nehorai, A. (2001). Cramer-Rao bounds for estimating range, velocity, and direction with an active array. *IEEE Transactions on Signal Processing*, 49(6), 1122-1137.
[20] Friedlander, B. and Porat, B. (1989). Performance analysis of a null-steering algorithm based on direction-of-arrival estimation. *IEEE Transaction on Acoustics, Speech, Signal Processing*, 37(4), 461-466.
[21] Amin, M.G. (1992). Concurrent nulling and locations of multiple interferences in adaptive antenna arrays. *IEEE Transaction on Signal Processing*, 40(11), 2658-2668.